UNIVERSITA' DEGLI STUDI DI ROMA
"LA SAPIENZA"
Dipartimento di Fisica

A.G.I.
Associazione Geofisica
Italiana

S.I.M.A.
Societa' Italiana di Meteorologia
Applicata

"Atmospheric Physics and Dynamics in the Analysis and Prognosis of Precipitation Fields"

Rome, 15 - 18 November 1994

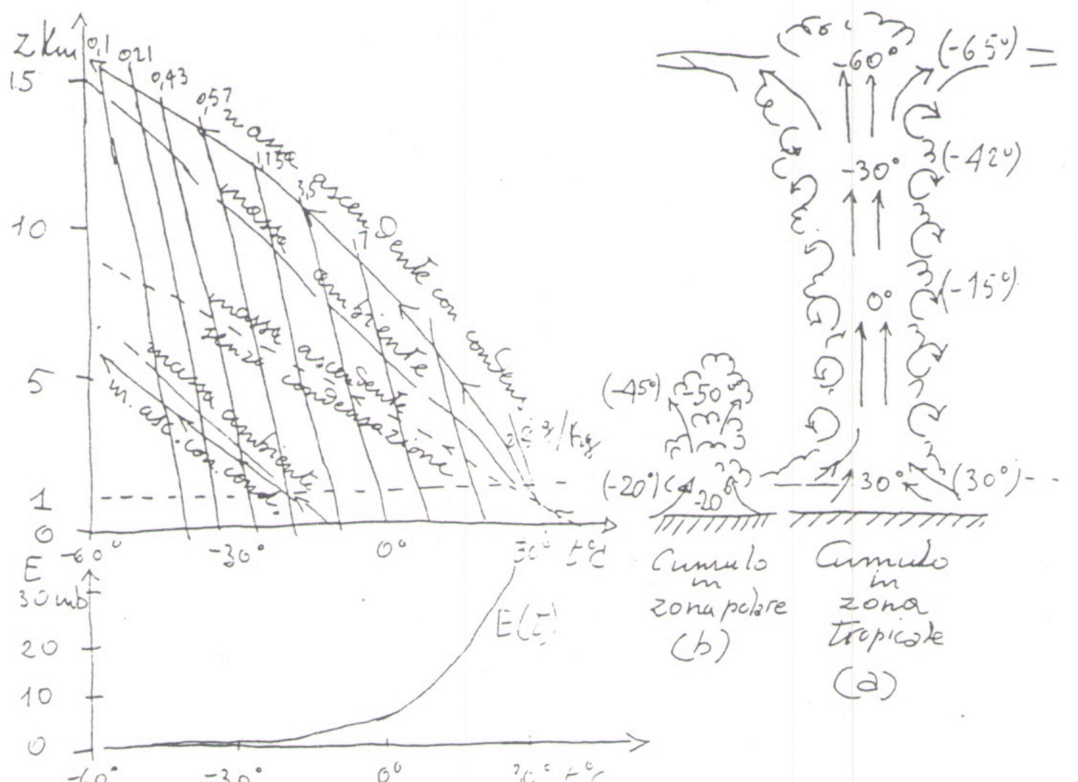

Massa d'aria satura in ascesa con condensazione all'equatore (a) e su zona polare (b)

Under the patronage of:
World Meteorological Organisation
Ministero dell'Università e della Ricerca Scientifica e Tecnologica

ATMOSPHERIC STRUCTURES COUPLED WITH LOCAL PRECIPITATION

F. Valero[1], C.García-Legaz[2], J.A. García-Miguel[1] , J.F.Gonzalez[1]
1 Complutense University of Madrid. Madrid. Spain
2 National Institute of Meteorology. Madrid. Spain

ABSTRACT
A methodology is carried out to show relationships between atmospheric structures and daily precipitation over the Comunidad Autonoma de Madrid (CAM) by isolating coupled coherent precipitation patterns by means of singular decomposition analysis (SDA).

1.INTRODUCTION

This paper deals with the development of a methodology to show the relationships between atmospheric structures and daily rainfall totals over the Comunidad Autonoma de Madrid (CAM). The study performed through a rotated principal components analysis (RCPA) allows us to segregate the spatial study domain into subregions whose rainfall amounts exhibit unique, homogeneous characteristics, presumably in response to a communality of forcing (i.e. local meteorology, upper-air conditions, orography, ...). Regionwide precipitation indicators are developed.

2.DATA

Daily rainfall data gathered during 1990 by a network operated by the National Meteorology Institute in the Comunidad Autonoma de Madrid were used as the basis for this study. The initial number of stations is 50. However, the scattering of the original stations is far from uniform and not the best suited to carry out the analysis of an area subdivided by eigenvectors. This is why those stations that supplied redundant information have been removed. In order to discard the redundant stations, a correlation matrix of all the stations was determined and a threshold (0.8) value of the correlation coefficient was fixed. Based on this procedure a network of 35 stations was finally selected that shows a fairly uniform spatial distribution. The aerological values used in this study were determined from the TEMP meteorological reports of the radiosonde station located in Barajas (Madrid).

3.COHERENT PRECIPITATION STRUCTURES

A Singular Descomposition Analysis (SDA) (Rasmusson *et al.*, 1981) has been carried out to establish coherent precipitation structures, i.e., to characterize the space-time variability of rainfall in the CAM area. A set of intercorrelated variables is orthogonally transformed to one of non-correlated independent variables or eigenvectors. Therefore, the procedure is based in the diagonal arrangement of the covariance matrix to find its eigenvalues and eigenvectors. The eigenvectors are linear combinations of the original variables while their respective eigenvalues are associated with explained variance corresponding to the respective eigenvector. If only the first pairs of eigenvalue-eigenvectors are selected, a substantial part of the total variance can be explained discarding the components of highest order that may be regarded as noise. When this process is applied to the daily rainfall data of the already mentioned network three significant eigenvectors were found by Rule N (Craddock and Flood, 1969). Percentages of 60, 8 and 4% were explained respectively by these three eigenvectors. The spatial plotting of these eigenvectors is shown in Figure 1. A dorsal-like pattern with its SW-NE axis separating two zones that show minimum rainfall, can be seen in Figure 1, one on that part of the CAM of significant orography and the other in the SE area. A structure, clearly different from the previous one, can be seen in Figure 1, that shows positive rainfall anomalies towards the N-NW of the CAM. Figure 1 is representative of the opposite phase of the first structure, i.e., a trough or central band with a SW-NE axis, that separates maximum values in the NW and SE zones.

For studying each of the eigenvectors, one specific day selected from the data base being used, was assigned to each of them. The Molteni method (Molteni *et al.*, 1983) was applied here. In this way, the first eigenvector was associated to the 21/11 day, the second to the 28/10 and the third to the 23/3. The rainfall efficiency (ratio as daily rainfall and the precipitable water amount) (Saucier, 1955) is shown in Figure 2 for these days. The spatial distributions of this ratio (in tens of %) are shown in this figure computed for the representative days of each eigenvector. In the first illustration (Figure 2), it can be seen that, for the day of maximum signal in the first eigenvector (W = 17 mm), the associated precipitation process projects the precipitacion over the entire spatial domain, except for the northeastern area of the region, and outlines two zones of maximum efficiency (about 40%)

: SW and NE showing a tendency to lie on the band of maximum precipitation anomaly of the first ector (with an average efficiency of 16.2%). A significant efficiency maximum is highlighted in Figure 2 for the orography zone (western edge of the region) exhibiting a marked gradient. The trend of this pattern to match the second eigenvector (W = 30 mm), is also evident. In this case, the rainfall distribution is rather less uniform that in the first case since rainfall in the southern zone is almost non-existent. This pattern shows a higher average rainfall efficiency (24%) conditioned by the orographic effect. As regards the third situation of Figure 2, a rather uniform efficiency of rainfall can be seen (with 66 mm of estimated precipitable water) in the complete domain, except for the higher orography zone in the northern part of the CAM where the average efficiency is of 23%.

Associated atmospheric structures

The temperature and dew-point profiles for the day selected as representative of the ***first eigenvector*** are shown in Figure 3*a* in an skew-T diagram by thick solid and thick but dashed tracings, respectively. The main feature is a rather small convective available potential energy (CAPE) value (9.67 J/Kg) showing the non-convective nature of rainfall. The equilibrium level (EL) and lifting condensation level (LCL) are 2,617 m and 836 m respectively; the level of free convection (LFC) is sited at 1593 m, 487 m above the convective condensation level (CCL). These are typical values for winter soundings, and they are characterized by a layer of comparatively dry air at the lower levels from surface up to 750 mb. In this region, the temperature lapse rate is smaller than the adiabatic one but similar to the saturated one resulting in a situation of relative conditional instability. Above 700 mb, a strongly stable layer of thickness somewhat less than 100 mb is found. This is a comparatively humid layer, as shown by the small depression of the dew-point (less than 2°C). Above 600 mb, the atmosphere becomes drier, so that if forcing out exists (e. g. a front) pushing air upwards an convective instability could then be posible. The rather uniform precipitation as well as the small estimated CAPE seem to point out that the convective activity, linked to this eigenvector, is negligible and so rainfall has to be of synoptic nature and probably associated to front disturbances. A front moving across the Peninsula can be seen in the synoptic chart (not shown here). From the vertical sounding (Figure 3*a*) cold advection characterized by backing of the wind below 500 mb is apparent as well as weak warm advection characterized by veering above 500 mb. Baroclinic conditions linked to sizeable vertical wind shear are brought by a jet stream that goes across the Peninsula virtually encompassing the same area than that of the frontal layer at the lowest levels. The maximum rainfall efficiency spread over an E-SE axis as can be seen in Figure 2*a*. This direction matches that of the wind just below the inversion in the layer of conditional instability and, therefore, in that part of the atmosphere where the cloudiness layer was located.

As regards the representative day of the ***second eigenvector***, the temperature and dew - point profiles are shown in Figure 3*b*. The temperature structure is characterized by a rather small (0.01 J/kg) CAPE meaning that convection is inhibited. The top (EL) and base (LCL) of the cloudiness is located around 2254 m and 901 m, respectively, while that of CCL is at 1359 m. Thus, stable conditions exist and precipitation may be clasified as stratiform. The deep, moist and highly stable layer between 800 and 500 mb is the most remarkable feature of this profile. Above this level, the dew-point depression increases slightly. The tropopause is located at a higher level than the previous case. It can be noticed again that the dew-point depression, at this level, is not very significant. For the mentioned reasons, the upper troposphere and lower stratosphere are comparatively humid due, as in the previous case, to the atlantic origin of the air masses. In Figure 2*b*, a regionwide scope of rainfall, in the N-NW area of the CAM was shown by the second eigenvector with maximum loadings near the Navacerrada Pass. This seemed to suggest that rainfall was heavily conditioned by the orography. The surface chart shows an instability line involving warm advection of maritime air. A strong jet stream going across the Peninsula from NW to SE is noticed at upper levels. The veering of wind (Figure 3*b*) shows warm advection virtually at all levels. The thickness of the moist layer results from moist advection. The jet is sited around 550 mb (halfway in this layer). On the other hand, the NW wind at 800 mb, in the zone of expected cloudiness formation, accounts for the location of maximum precipitation in the N and NW area of the CAM, since the orography would promote cloudiness formation and precipitation. It should be kept in mind that an air layer in nearly-saturated conditions may provide the "fuel" for triggering convective rainfall. Föhn effect could explain the strong gradient of rainfall efficiency that can be seen in Figure 2*b*.

Finally, the sounding corresponding to the **third eigenvector** is shown in Figure 3*c*. This structure isolated by singular decomposition is characterized by a low CAPE (28.41 J/kg), although higher than that of previous cases. This value, although small, suggests a certain degree of "convectivity" in the atmosphere and, therefore, the nature of the precipitation associated to this eigenvector has to be still more convective than those for previous cases. The top (4085 m) and base (1554 m) of the clouds, the CCL at 2071 m and the LFC at 2783 m yield an estimated cloud thickness of 2500 m larger than the corresponding estimates for the two other cases. This structure is, generally speaking, more unstable than those determined by previous soundings. But for a small isothermal layer around 900 mb, the geometric lapse rate from ground to 700 mb is near the adiabatic lapse rate involving neutral stability. In this layer, the dew-point depression is comparatively high and would indicate that comparatively dry air is present. In the 700/500 mb and 400/300 mb layers, the geometric lapse rate matches, on the average, the saturated adiabatic one. Dew-point depressions between surface and upper tropospheric levels exceeds that of previous soundings. Therefore, the potential or convective instability is more significant in this type of soundings.

The precipitation efficiency associated to this third eigenvector (Figure 2*c*) was targetted in the northern zone of the CAM while comparatively low efficiencies were shown at the remaining areas. The lack of a significant efficiency gradient, as that for the second eigenvector, as well as the substantially larger CAPE seem to suggest that rainfall is not mainly determined by the orography, although, it may explain the maximum efficiency in this region. It could be said that rainfall associated to this eigenvector is more convective than in the previous situations and orography acts as an amplifier for transforming in rainfall any water available in the atmosphere. The surface chart shows the atlantic anticyclone advancing into Europe with lower pressures over Iberia. This low pressures appear to have a thermal origin since the surface temperature are abnormally high for the season of the year being. An unexpected setting in of the circumpolar vortex is noticed at upper levels, in the shape of a trough, with the axis running NE-SW and a cold air pool, as found by soundings (Figure 3*c*), due to the tropopause collapse. Winds are virtually absent due to the low pressure gradient noticed at ground level. This fact coupled with a jet stream passing above the Iberian Peninsula generates a "suction" effect that could act as a dynamic "triggering" system that can develop local storms.

Summarizing, this eigenvector shows an efficiency distribution of precipitation associated to the joint effect of both a dynamic and orographic forcing acting on the thermal structure that shows neutral stability and/or potential or convective instability.

4.CONCLUDING REMARKS

Daily precipitation data for the Comunidad Autonoma de Madrid suplied by the National Meteorology Service have been studied in order to asses the existence of spatial patterns coupled with specific atmospheric structures. Three rainfall patterns accounting for a high percentage (72%) of rainfall variability in the studied area were isolated. These three patterns involve maximum precipitation efficiency in three distinctly different areas:

Pattern 1 associated to a maximum precipitation efficiency over the central region of the CAM. Its average efficiency is 16%, and it is distributed uniformily throughout the CAM except for the north-western corner). The precipitable water involved is estimated to be 17 mm. The associated atmospheric structure consists of a cold front passing through the Peninsula and characterized by cold lower - layer advection with SW flows at 700 mb level and upwards that would generate stratiform cloudiness.

Pattern 2 associated to a maximum precipitation efficiency over the north-western region region of the CAM. Its average efficiency is 24% showing an enhanced eficiency gradient towards the NW. The precipitable water involved is estimated to be 63 mm. The associated atmospheric structure consists of an incipient warm front over the Peninsula with warm advection nearly at all levels. This situation involves stable atmospheric conditions . The orography seems to be a forcing factor for precipitation.

Pattern 3 associated to a maximum precipitation efficiency over the north region of the CAM with 23% average efficiency showing a weaker gradient towards the NW. The precipitable water involved is estimated to be 66 mm. The associated atmospheric structure consists of a thermal low at lower levels combined with an unexpected setting in of the circumpolar vortex at upper levels. This situation involves stable atmospheric conditions. The orography seems to be a forcing factor for precipitation.

5.REFERENCES

Craddock, J. M. and C. R. Flood, Eigenvectors for representing the 500 mb geopotencial surface over the northern hemisphere. Quart. J. Roy. Meteor. Soc., 95, (1969) 576-593.

Molteni, F., P. Bonelli and P. Bacci, Precipitation over northern Italy: a description by means of principal components analysis. J. Appl. Meteor., 22, (1983) 1738-1752.

Rasmusson, E. M. , P. A. Arkin, W-Y Chen and J. B. Jalickee, Biennal variations in surface temperature over the United States as revealed by singular decomposition. Mon. Wea. Rev., 109, (1981) 587-598.
Saucier W. J., Principles of Meteorological Analysis. University of Chicago Press, Chicago (1955) 438 pp.

FIGURE 1

FIGURE 2

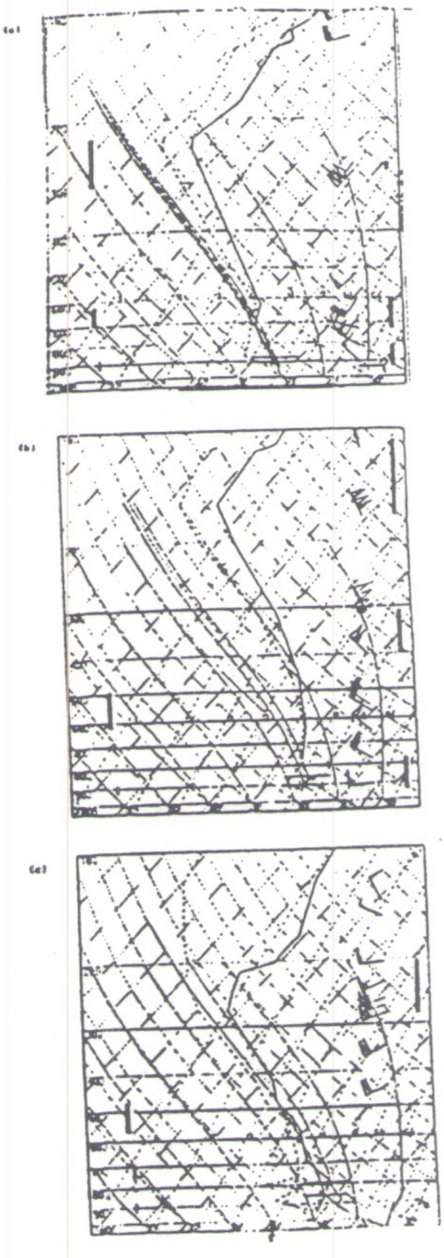

FIGURE 3

Fig. 1. (a) First, (b) second, and (c) third eigenvector patterns of daily precipitation.
Fig. 2. (a) First, (b) second, and (c) third eigenvector patterns of daily precipitation efficiency.
Fig. 3. Air temperature (solid line) and dew temperature (dashed line) soundings in a skewed-T and logaritmic preassure diagram for the three selected case studies.